

Demethoxycurcumin in combination with ultraviolet radiation B induces apoptosis through the mitochondrial pathway and caspase activation in A431 and HaCaT cells

Tumor Biology

June 2017: 1–11

© The Author(s) 2017

Reprints and permissions:

sagepub.co.uk/journalsPermissions.nav

DOI: 10.1177/1010428317706216

journals.sagepub.com/home/tub

Yong Xin¹, Qian Huang¹, Pei Zhang¹, Wen Wen Guo¹,
Long Zhen Zhang¹ and Guan Jiang²

Abstract

Photodynamic therapy is widely used in the clinical treatment of tumors, especially skin cancers. It has been reported that the photosensitizer curcumin, in combination with ultraviolet radiation B, induces HaCaT cell apoptosis, and this effect may be due to the activation of caspase pathways. In this study, we examined the photodynamic effects of demethoxycurcumin, a more stable analogue of curcumin, to determine whether it could induce apoptosis in skin cancer cells. We investigated the effects of a combination of ultraviolet radiation B and demethoxycurcumin on apoptotic cell death in A431 and HaCaT cells and determined the molecular mechanism of action. Our results showed increased apoptosis with a combination of ultraviolet radiation B with demethoxycurcumin, as compared to ultraviolet radiation B or demethoxycurcumin alone. The combination of ultraviolet radiation B irradiation with demethoxycurcumin synergistically induced apoptotic cell death in A431 and HaCaT cells through activation of p53 and caspase pathways, as well as through upregulation of Bax and p-p65 expression and downregulation of Bcl-2, Mcl-1, and nuclear factor- κ B expression. In addition, we found that reactive oxygen species significantly increased with treatment, and mitochondrial membrane potential depolarization was remarkably enhanced. In conclusion, our data indicate that demethoxycurcumin may be a promising photosensitizer for use in photodynamic therapy to induce apoptosis in skin cancer cells.

Keywords

Demethoxycurcumin, photodynamic therapy, apoptosis

Date received: 6 December 2016; accepted: 13 March 2017

Introduction

Cutaneous squamous cell carcinoma (cSCC) is a common malignant skin cancer originating in epithelial cells.¹ It is the second most common form of skin cancer, following basal cell carcinoma (BCC).^{2,3} The incidence of cSCC has risen in recent decades, increasing by 10% on a yearly basis.⁴ cSCC originates in the epidermis or adnexal keratinocytes and occurs mainly on the scalp, face, and back of the hand.⁵ The primary cause of cSCC is exposure to ultraviolet radiation, which causes DNA damage in keratinocytes.^{6,7} cSCC is characterized by a complicated etiology, a high rate of clinical misdiagnosis, a high degree

of malignancy, and a high level of invasion and cellular damage.

Traditional methods of treatment for skin cancer include surgery, radiation therapy, chemotherapy, photodynamic

¹Department of Radiotherapy, Affiliated Hospital of Xuzhou Medical College, Xuzhou, China

²Department of Dermatology, Affiliated Hospital of Xuzhou Medical College, Xuzhou, China

Corresponding author:

Guan Jiang, Department of Dermatology, Affiliated Hospital of Xuzhou Medical College, Xuzhou, Jiangsu 221002, China.

Email: dr.guanjiang@gmail.com



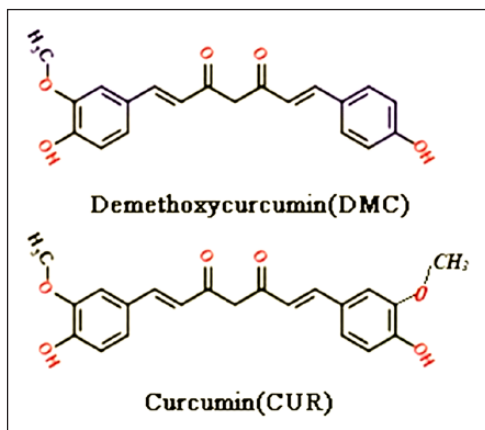


Figure 1. Structures of curcumin and DMC. In comparison to curcumin, the structure of DMC lacks a methoxy group.

therapy (PDT), and biological therapies.⁸ Early surgical intervention is the first choice for treatment for malignant skin tumors; however, the large extent of resection often results in scarring or changes in appearance of the affected area, increasing the psychological burden for patients. Long-term chemotherapy can lead to gastrointestinal reactions and drug resistance, require patients to undergo bone marrow transplantation, or cause other adverse reactions. Local radiation therapy can lead to the formation of free radicals, causing local inflammation of the skin manifested as exudation, dermatitis, peeling, and ulcers.⁹ Long-term treatment can even result in fibrosis, necrosis and secondary tumor formation, or other adverse reactions.¹⁰ Therefore, it is important to choose a safe and effective approach to treat skin cancer.

PDT is a treatment involving light-induced activation of photosensitizers in the presence of oxygen, resulting in the production of free radicals capable of inducing cell death. In recent years, PDT has become an established treatment for selected neoplastic lesions, especially skin cancers, including BCC, squamous cell carcinoma, actinic keratosis, Bowen's disease, extramammary Paget's disease, and precancerous lesions.^{11–14} PDT, like many chemical and physical treatments capable of inducing apoptosis, is known to provoke oxidative stress by generating reactive oxygen species (ROS) in cells, suggesting a close relationship between oxidative stress and apoptosis. Currently, one of the main factors limiting photodynamic effects is the photosensitizing agent.¹⁵

Curcumin and demethoxycurcumin (DMC) are derived from the rhizome of the plant *Curcuma longa* (turmeric) and collectively referred to as curcuminoids (Figure 1).¹⁶ The stability of DMC is higher than that of curcumin, which prevents lipid peroxidation.¹⁷ In recent years, many studies have shown that DMC and curcumin can modulate multiple cell signaling pathways, including apoptosis.^{18–20} Based on these studies and its structure and function, we hypothesized that DMC may likewise act as a photosensitizer.

To further explore this possibility, we investigated the photodynamic effects of DMC to determine whether the combination of ultraviolet radiation B (UVB) and DMC could induce apoptotic cell death in the A431 and HaCaT cell lines. The study of apoptosis induced by PDT is mainly focused on mitochondrial pathway and the death receptors. In addition, caspase receptor family is one of the most important death receptors. PDT induced endoplasmic reticulum stress, resulting in apoptosis, is still in the exploratory stage. So, we choose to study the mitochondrial pathway and caspase pathway. In mitochondrial pathway, ROS produced during photodynamic reaction damage the structure of DNA molecular and activate mitochondria, thus inducing cell apoptosis.²¹ In caspase pathways, when mitochondrial function is destroyed, cytochrome C is released and then mediates a series of caspase family apoptotic cascades.²²

Results

DMC and UVB reduce tumor cell viability in a dose-dependent manner

Before initiating experiments involving a combination of DMC and UVB, we assessed the effects of DMC and UVB alone on the growth of A431 and HaCaT cells. Treatment of cells with various concentrations of DMC results in a dose- and time-dependent increase of cell inhibition rate ($p < 0.05$; Figure 2(a) and (b)). Inhibition of A431 cell proliferation is observed starting at 10 $\mu\text{mol/L}$, whereas inhibition of HaCaT cells occurs at 20 $\mu\text{mol/L}$, and inhibition increases with time, peaking at the third day (72 h).

Similar to DMC, UVB inhibits cellular proliferation in a dose-dependent manner ($p < 0.05$; Figure 2(c)). Inhibition increases with an increasing dose of irradiation in the range of 10–70 mJ/cm^2 . At 50 mJ/cm^2 , inhibition of proliferation of A431 cells is 49.94%, while for HaCaT cells inhibition is 41.92%. The inhibitory peak is reached at 70 mJ/cm^2 . These results show that both DMC and UVB reduce tumor cell viability in a dose-dependent manner.

Inhibition of tumor cell growth is enhanced by treatment with DMC plus UVB

To determine whether combining DMC and UVB would enhance inhibition of cell proliferation, A431 and HaCaT cells were treated with DMC plus UVB. Based on the observed dose response curves of DMC (5–80 μM) and UVB (10–100 mJ/cm^2) in Cell Counting Kit-8 (CCK-8) assays that show the sum of necrotic cells and apoptotic cells, we chose half the maximum dose in order to detect the combined effects of DMC and UVB, resulting in a dose of 40 $\mu\text{mol/L}$ DMC and 50 mJ/cm^2 UVB. As shown in Figure 2(d), treatment of cells with a combination of a fixed concentration of DMC (40 $\mu\text{mol/L}$) and fixed dose of UVB (50 mJ/cm^2) produced higher inhibition compared to treatments with single

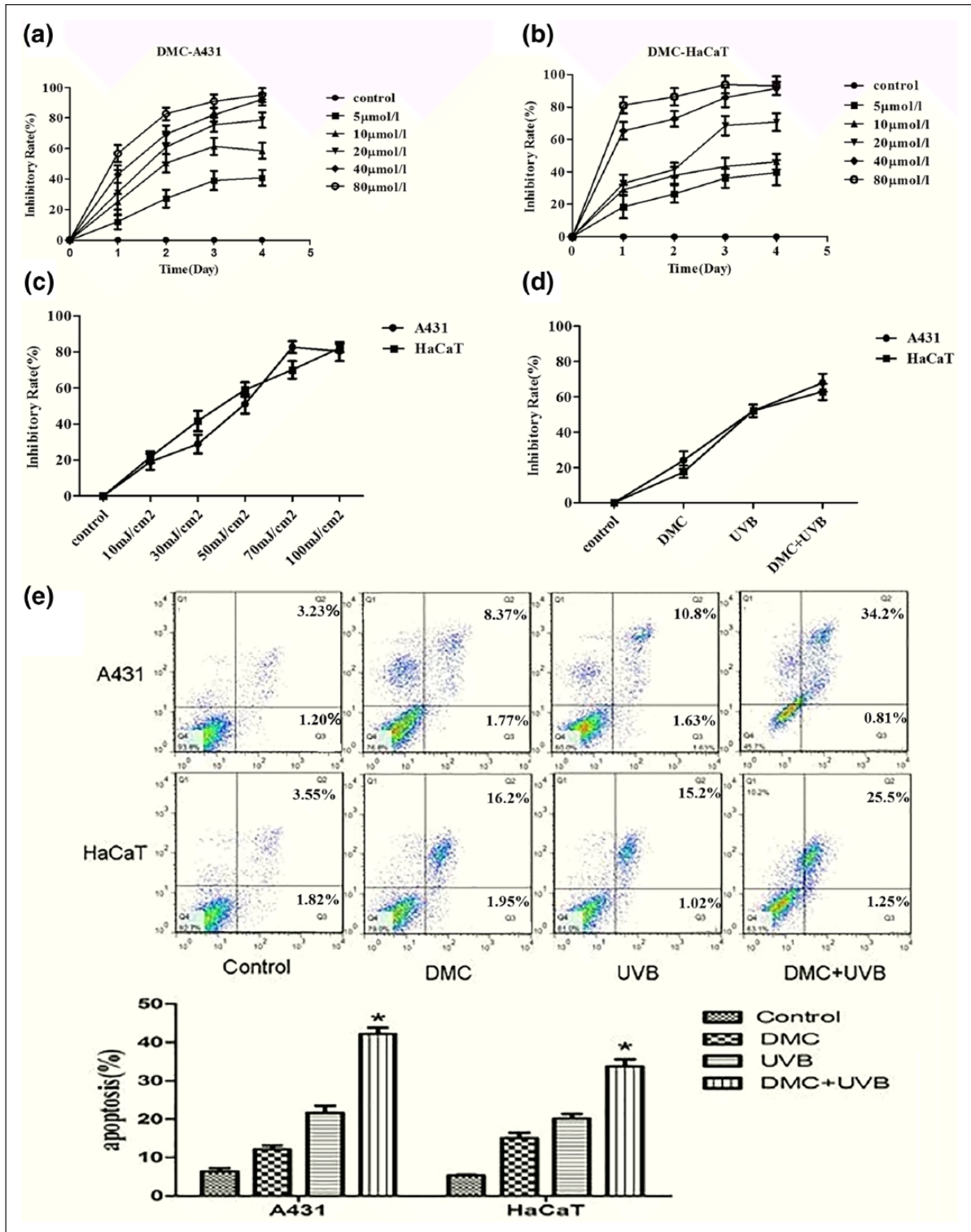


Figure 2. Effects of DMC, UVB, or DMC/UVB on the growth of A431 and HaCaT cells. (a) CCK-8 assay of A431 cells treated with DMC (5, 10, 20, 40, and 80 $\mu\text{mol/L}$) after 1, 2, 3, and 4 days of treatment. (b) CCK-8 assay of HaCaT cells treated with DMC (5, 10, 20, 40, and 80 $\mu\text{mol/L}$) after 1, 2, 3, and 4 days of treatment. (c) CCK-8 assay of A431 and HaCaT cells treated with UVB (10, 30, 50, 70, or 100 mJ/cm^2). (d) CCK-8 assay of A431 and HaCaT cells treated with DMC (40 $\mu\text{mol/L}$) and UVB (50 mJ/cm^2). The DMC group was treated with 40 $\mu\text{mol/L}$ DMC for 2 h, the UVB group was irradiated with a dose of 50 mJ/cm^2 , and the combined group was pretreated with DMC for about 2 h and then irradiated with UVB at a dose of 50 mJ/cm^2 . Results are expressed as the mean \pm SD of three independent experiments. (e) Apoptotic changes in treated cells. A431 and HaCaT cells were treated with DMC plus UVB (40 $\mu\text{mol/L}$ and 50 mJ/cm^2 , respectively), DMC (40 $\mu\text{mol/L}$), or UVB (50 mJ/cm^2). Following treatment, cells were stained with FITC-labeled annexin V/PI and analyzed by flow cytometry. Data are presented as mean \pm SD of the percentage of annexin-positive cells from three independent experiments (* $p < 0.05$ vs DMC- or UVB-treated groups; $n = 3$).

agents alone or untreated control cells ($p < 0.05$). The control cells were cultured in Dulbecco's Modified Eagle's Medium (DMEM) supplemented with 10% fetal bovine serum (FBS) at 37°C in an atmosphere containing 5% CO₂. The combination treatment shows additive to synergistic therapeutic activity in reducing the number of tumor cells.

Enhancement of apoptosis in cells using a combination of DMC and UVB

Flow cytometry (FCM) analysis that shows apoptotic cells confirms that treatment with DMC, UVB, or combination of DMC and UVB results in apoptosis. Our data show that the rate of apoptosis in each treatment group in A431 cells is 4.43%, 10.14%, 12.43%, and 35.01% and in HaCaT cells the rate is 5.38%, 18.15%, 16.22%, and 26.75%. These results suggest that DMC, together with UVB treatment, additively or synergistically induces an increased number of cells to undergo apoptosis, compared to treatment with DMC or UVB alone ($p < 0.05$; Figure 2(e)).

DMC and UVB increase apoptosis in A431 and HaCaT cells through the mitochondria-mediated apoptosis pathway

To investigate whether the increased apoptosis during combination treatment with DMC and UVB was induced through activation of the mitochondria-mediated apoptosis pathway, we measured changes in mitochondrial potential and ROS levels following treatments in A431 and HaCaT cells. As shown in Figure 3(a) and (b), a remarkable increase in mitochondrial potential loss and ROS changes, an early indicator of mitochondria-mediated apoptosis,^{23–25} is observed in all experimental groups after treatment. The combination of DMC and UVB leads to an increase in mitochondrial potential loss and ROS in 75%–90% cells ($p < 0.05$). The increased loss in mitochondrial potential and ROS suggests that DMC in combination with UVB induces apoptosis by activating the mitochondrial pathway.

Morphological characteristics of apoptosis

To investigate the morphological characteristics of apoptosis, A431 and HaCaT cells were exposed to DMC (40 μmol/L), UVB (50 mJ/cm²), or DMC plus UVB and stained with Hoechst 33258 for observation using fluorescence microscopy. Control cells which did not undergo any experimental treatment were uniformly stained, with no substantial fluorescence signal. Shrinkage of cells was observed in A431 and HaCaT cell lines exposed to DMC, UVB, or the combination of DMC and UVB. The number of apoptotic cells increased and cells displayed typical changes associated with apoptosis more significantly in the combination treatment group than in the individual

treatment groups, including a reduction in the number of cells, bright staining, and fragmented nuclei (Figure 3(c)).

Effects of the combination of DMC and UVB on apoptosis-associated proteins including Bcl-2, Mcl-1, Bax, nuclear factor-κB (p65), p-p65, p53, caspase-3, caspase-9, and cytochrome c

To study the photodynamic effects of DMC, cells were exposed to sub-apoptotic doses of UVB (50 mJ/cm²) and cultured in media with a DMC concentration insufficient to cause apoptosis (40 μmol/L). Cells were harvested following irradiation for western blotting. Activation of p53, Bax, caspase-3, and caspase-9 is apparent following treatment with the combination of UVB and DMC, but only slight activation occurs with UVB or DMC treatment alone (Figures 4(a), (b) and 6(a)). Our results also showed that Bcl-2, Mcl-1, and nuclear factor-κB (NF-κB) proteins were decreased in the combined treatment group as compared to UVB- or DMC-treated cells (Figure 4(a) and (b)). Additionally, we examined the expression of activated NF-κB (p-p65) in the nucleus, which was higher in cells treated with the combination of UVB and DMC as compared to treatment with UVB or DMC alone (Figure 5). Furthermore, we observed that the levels of cytosolic cytochrome c were higher in the DMC plus UVB-treated cells than in UVB- or DMC-treated cells (Figure 6(a)).

Discussion

The incidence of cSCC has increased significantly over the past 20 years, and it is estimated that it will increase even further in the coming decade based on epidemiological studies.^{26,27} With the incidence of skin cancers and mortality attributed to the disease increasing globally, existing treatments do not significantly prolong survival. While early surgical treatment can completely remove the tumor, the remaining scar can cause significant discomfort to patients. Radiation therapy and chemotherapy both have varying degrees of side effects. PDT has been indicated as a promising treatment for the selective destruction of cancerous and non-neoplastic cells. This approach involves the simultaneous presence of light, oxygen, and a light-activatable chemical known as a photosensitizer. Curcumin as photosensitizing agent has been validated by many studies; however, curcumin has poor solubility and stability in aqueous solutions and undergoes rapid metabolism and systemic elimination.^{28,29} DMC is a curcuminoid with more stable physicochemical properties compared with curcumin. It has been shown that DMC possesses anticancer activity,^{30,31} antioxidant activity,³² and the ability to inhibit activation of microglial cells;³³ however, the effect of DMC on the dynamics of light has not yet been reported.

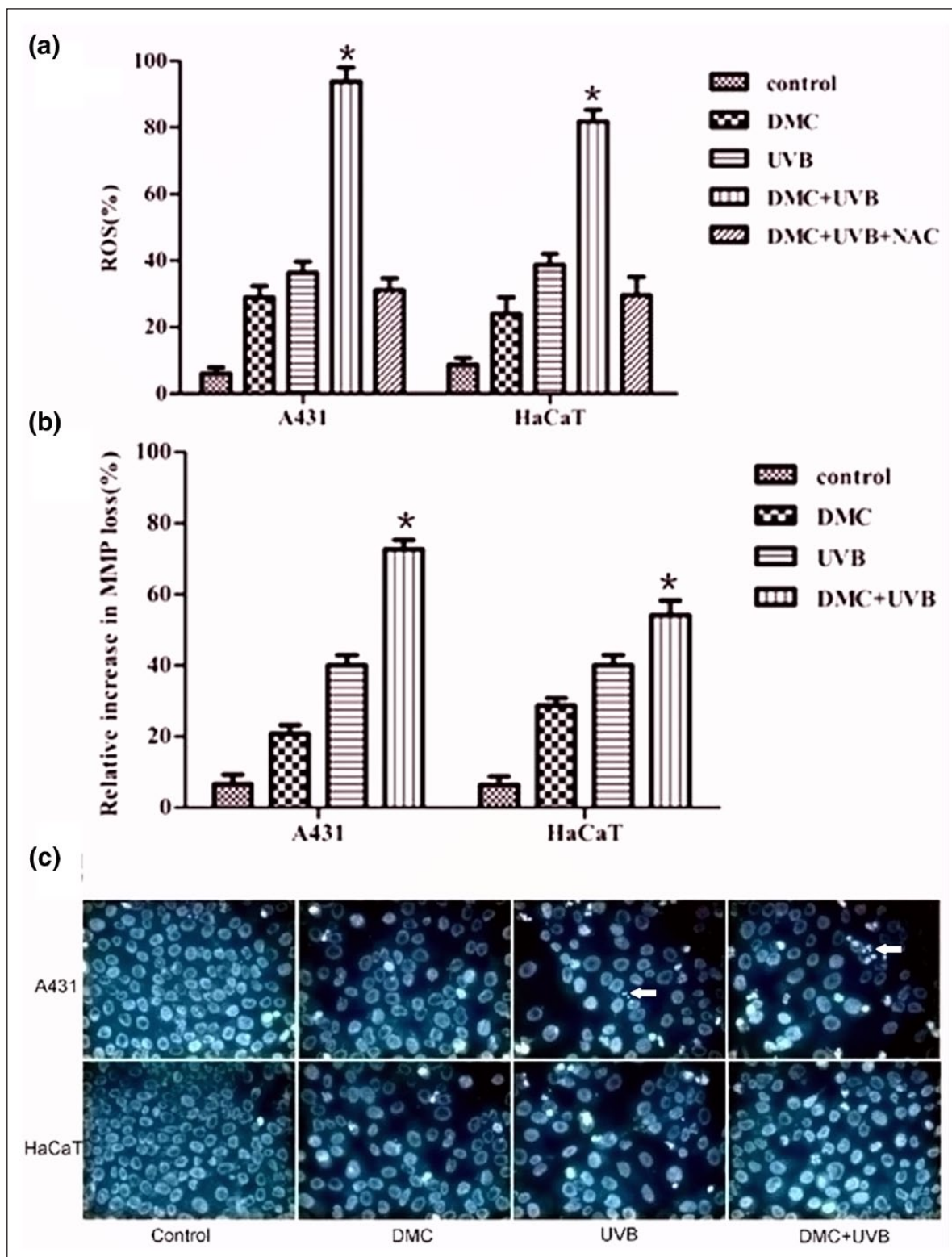


Figure 3. (a) ROS and mitochondrial potential changes following DMC and UVB treatment. A431 and HaCaT cells were treated with DMC plus UVB (40 $\mu\text{mol/L}$ and 50 mJ/cm^2 , respectively), DMC-PDT plus NAC (40 $\mu\text{mol/L}$, 50 mJ/cm^2 , and 5 mmol/L , respectively), DMC (40 $\mu\text{mol/L}$), or UVB (50 mJ/cm^2) and harvested and stained with DCFH-DA or Rhodamine 123 and analyzed by flow cytometry. (b) Data are expressed as mean \pm SD of the percentage of cells showing increased loss in mitochondrial potential (* $p < 0.05$ vs DMC- or UVB-treated groups; $n = 3$). (c) Morphological changes of the nuclei following treatment with DMC and UVB. A431 and HaCaT cells were treated with DMC plus UVB (40 $\mu\text{mol/L}$ and 50 mJ/cm^2), DMC (40 $\mu\text{mol/L}$), and UVB (50 mJ/cm^2). Following treatment, cells were incubated with Hoechst 33258, and nuclei condensation and fragmentation observed under a fluorescence microscope (original magnification 400 \times).

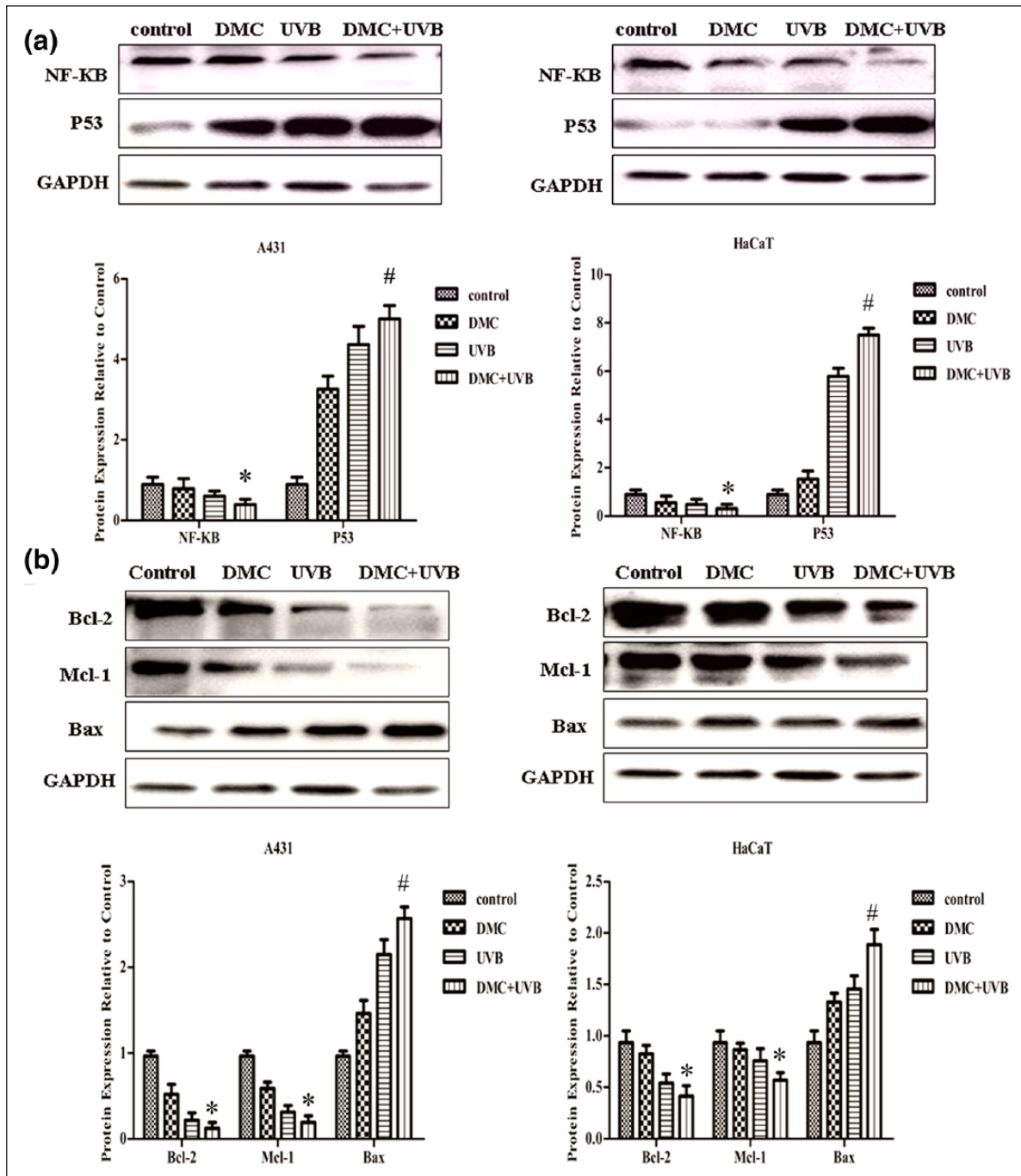


Figure 4. DMC/UVB treatment regulates (a) NF- κ B and p53 expression as well as (b) Bcl-2, Mcl-1, and Bax expression (* $p < 0.05$ and # $p < 0.01$ vs DMC- or UVB-treated groups; $n = 3$).

Oxygen-free radicals can initiate mitochondrial depolarization and increase the permeability of the mitochondrial membrane, causing mitochondrial swelling, rupture of the outer membrane, and release of cytochrome *c* into the cytosol. As an apoptosis-inducing factor, cytochrome *c* can form an apoptotic complex with Apaf-1, caspase-9 precursor, and adenosine triphosphate (ATP)/deoxyadenosine triphosphate (dATP) and then assemble and activate caspase-3, triggering a cascade that leads to apoptosis.

NF- κ B mainly localizes to the cytoplasm and is involved in regulation of proliferation and apoptosis in various cell types.^{34–36} The NF- κ B signaling pathway plays a key role in tumor occurrence and development, which contributes to the occurrence of cancer.^{37,38} When cells are in a non-stimulated state, NF- κ B combines with its inhibitor I κ B in an inactive form in the cytoplasm. When cells are subjected to damage and other stimuli, I κ B is degraded, and activated NF- κ B is released and transferred to the nucleus to regulate

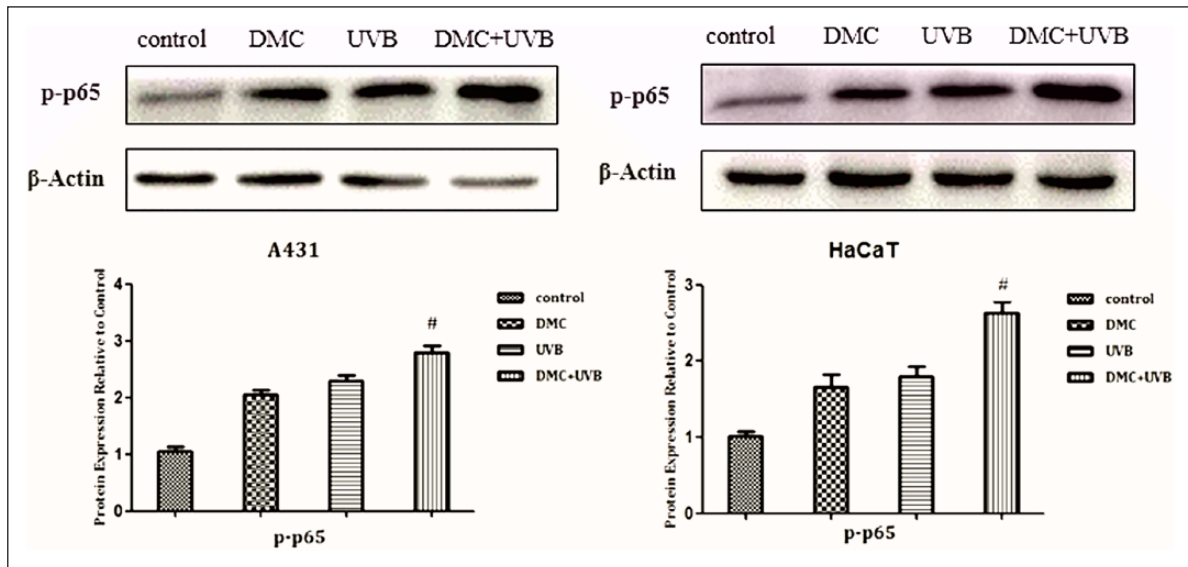


Figure 5. DMC/UVB treatment regulates p-p65 expression (* $p < 0.05$ and # $p < 0.01$ vs DMC- or UVB-treated groups; $n = 3$).

the transcription of target genes.³⁹ The p65 protein is a member of the NF- κ B family. It has been shown that inactivation of the p65 subunit leads to the death of liver cells by apoptosis.⁴⁰ Bcl-2 family proteins serve as critical regulators of pathways involved in apoptosis which can be classified into antiapoptotic and proapoptotic groups.^{41,42} The antiapoptotic group includes Bcl-2, Bcl-XL, Bcl-W, Mcl-1, and CED9 among others, while the proapoptotic group includes Bax, Bak, Bcl-XS, Bad, Bik, Bid, and others. Bcl-2 and Mcl-1 are genes downstream of NF- κ B. The ratio of Bax to Bcl-2^{43,44} determines cell apoptosis or survival. In addition, interactions between Bid, Bax, and Bak can trigger the release of proapoptotic molecules from the mitochondria, such as Cyto-*c*, AIF, EndoG, Samc/DIA-BLO, and Omi/HtraA2, and result in activation of apoptosis via the mitochondrial pathway.⁴⁵ The release of cytochrome *c* is closely associated with apoptosis. Caspases, a family of cysteinyl aspartate-specific proteases, play an essential role in the regulation and execution of apoptotic cell death.⁴⁶ Cytochrome *c* interacts with caspase-9 to form an apoptotic complex. This facilitates caspase-9 autoactivation,⁴⁷ activation of caspase-3, and other caspase members in the presence of ATP or dATP, which promotes apoptosis.^{48,49} Caspase-3 is the most extensively studied apoptotic protein. Under normal conditions, inactive caspase-3 is localized to the cytoplasm. Apoptotic signals can lead to proteolytic cleavage and activation of caspase-3.⁵⁰⁻⁵³ Activation of caspase-3 and downstream substrate cleavage results in a cascade of proteolytic amplification and ultimately leads to the death of the cell.⁵³

In our study, we focused on the NF- κ B survival pathway, the generation of ROS, depolarization of the mitochondria, and mitochondrial membrane permeability and examined Bcl-2, Mcl-1, Bax, p53, and caspase-3 pathways to analyze the potential molecular mechanisms leading to apoptosis.

In this study, we used different doses of DMC and UVB on A431 and HaCaT cells, and based on CCK-8 assays, DMC and UVB could inhibit the proliferation of A431 and HaCaT cells and showed a significant dose-effect relationship. To further understand the effect of DMC as a photosensitizer, we combined DMC with UVB, treated A431 and HaCaT cells, and monitored the effects on cells by CCK-8 assays, FCM, cell morphology, ROS, and western blotting. The results of western blotting showed that Bax, p53, caspase-3, caspase-9, p-p65, and cytochrome *c* proteins were higher in the combined treatment group, while Bcl-2, Mcl-1, and NF- κ B proteins were decreased in the combined treatment group. Therefore, by analyzing the expression of different proteins, the relationship between these proteins, the differences in cellular morphology, the changes in ROS, and mitochondrial membrane potential, we established that the mechanisms of UVB combined with DMC in the treatment of tumors may suppress proliferation and induce apoptosis via multiple cell signaling pathways, especially the mitochondrial pathway (Figure 7). Prior to our study, no research had examined the use of DMC as photosensitizer. Our study shows that a combination of UVB and DMC inhibits growth and amplifies proapoptotic effects. DMC not only has anticancer activity but also can be used as a new photosensitizer, which could be a novel therapeutic approach for photodynamic tumor therapy. UVB in combination with DMC is expected to be a new, effective method for the treatment of cSCC.

Currently, the basic research on PDT is relatively limited, and many issues remain to be addressed. Deficiencies exist in the research and development of photosensitive drugs. In clinical practice, because of the lack of understanding of laser propagation in tissue, the photochemical reaction induced by photosensitizer, heat dose distribution in tissue of various regions, and dose determination, the

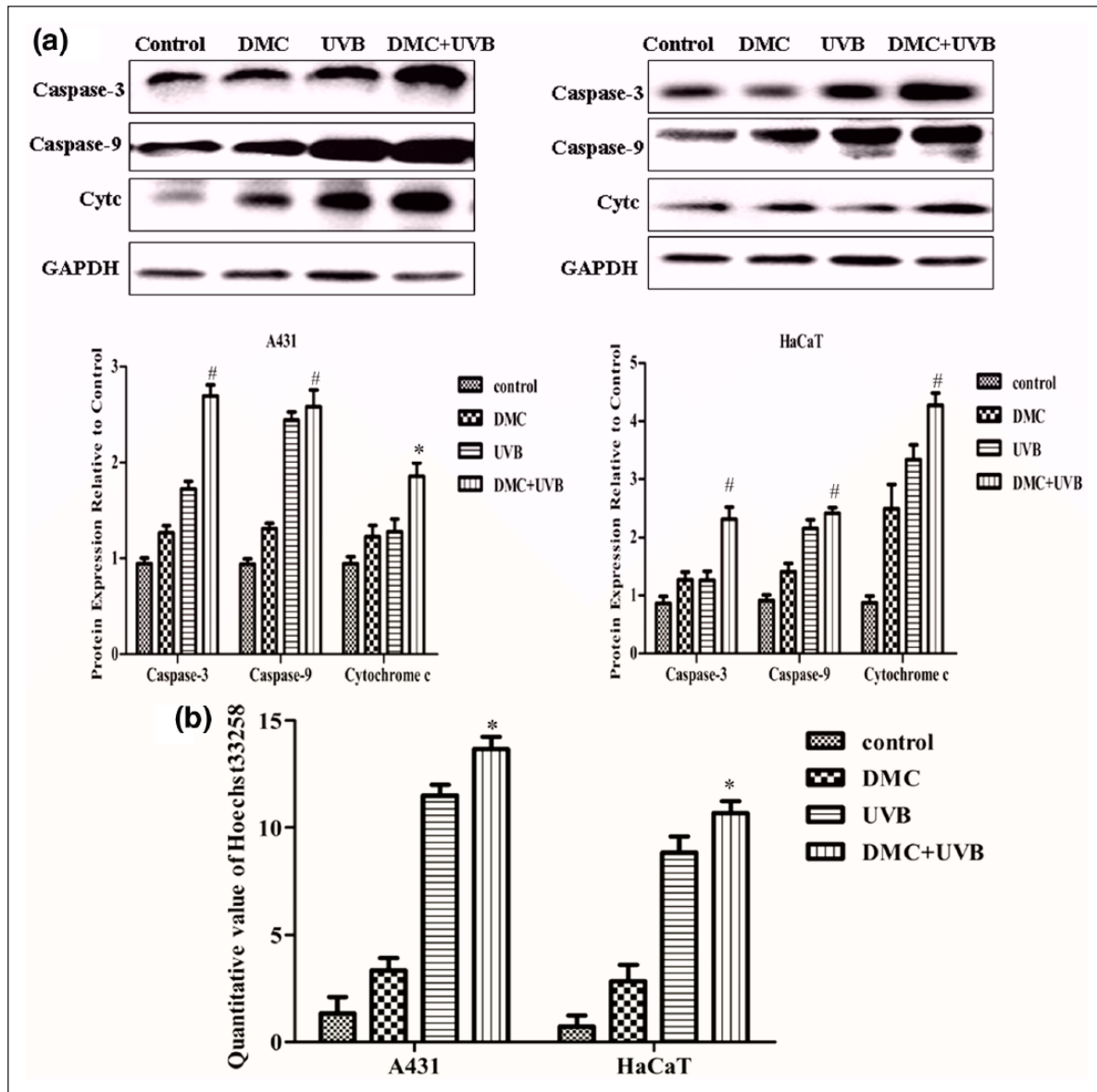


Figure 6. (a) DMC/UVB treatment regulates caspase-9, caspase-3, and cytochrome c expression. A431 and HaCaT cells were treated with DMC plus UVB (40 $\mu\text{mol/L}$ and 50 mJ/cm^2 , respectively), DMC (40 $\mu\text{mol/L}$), and UVB (50 mJ/cm^2). Untreated cells served as a negative control. Cell extracts were subjected to western blotting to detect caspase-9, caspase-3, and cytochrome c protein expression. GAPDH was used as a loading control. Quantitation of changes in band densities was performed using ImageJ analysis software, and changes are expressed as a ratio relative to levels in untreated cells, which were set to 1.0 (* $p < 0.05$ and # $p < 0.01$ vs DMC- or UVB-treated groups; $n = 3$). (b) Quantification of Hoechst 33258 staining.

application of PDT is not standardized and it has yet to play a role in the diagnosis and treatment of tumors. Further studies will be required to address these issues.

Materials and methods

Cells lines and culture conditions

The A431 epidermoid carcinoma cell line was purchased from the Shanghai Cell Bank of the Chinese Academy of

Sciences. The HaCaT keratinocyte cell line was obtained from Fuxiang Biotechnology Co., Ltd. (China). DMC (>99% purity) was obtained from YuanYe Biotechnology Co., Ltd. (China) and dissolved in dimethyl sulfoxide (DMSO) as a 100 mmol/L stock solution. The stock solution was stored at -20°C and diluted in complete medium before use. The final concentration of DMSO applied to the cells was less than 0.1%. Cell lines were cultured in DMEM supplemented with 10% FBS at 37°C in an atmosphere containing 5% CO_2 .

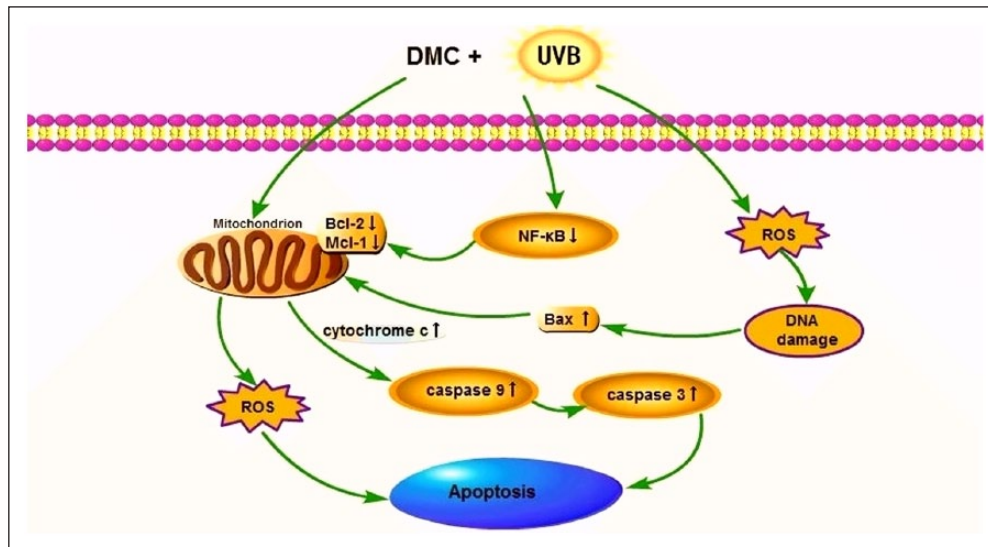


Figure 7. The possible cell signaling pathways involving UVB combined with DMC in the treatment of tumors.

Cell proliferation assay

To assess the inhibitory effects of DMC or UVB on the proliferation of A431 and HaCaT cells, 1×10^4 cells/well were seeded in 96-well plates and treated with various concentrations of DMC (5, 10, 20, 40, or 80 $\mu\text{mol/L}$) or UVB (10, 30, 50, 70, or 100 mJ/cm^2). After treatment, 10 μL of the CCK-8 solution (Vicmed Biotech Co. Ltd., China) was added to each well, followed by incubation for 2 h at 37°C. The absorbance was measured at 450 nm using an EMax Microplate Reader (Molecular Devices, USA).

To determine the combined effects of DMC and UVB on the viability of A431 and HaCaT cells, 1×10^4 cells/well were seeded in 96-well plates and treated with DMC (40 $\mu\text{mol/L}$), UVB (50 mJ/cm^2), or DMC plus UVB (40 $\mu\text{mol/L}$ and 50 mJ/cm^2 , respectively). Untreated cells served as controls. Cells were assayed for viability as described above. Experiments were conducted in triplicate, and the results were reported as the means of the three experiments.

Analysis of apoptosis

Apoptosis was measured using an Annexin V/propidium iodide (PI) apoptosis detection kit (Nanjing KeyGen Biotech, China) according to the manufacturer's instructions. Briefly, cells in each group were trypsinized, centrifuged (2000 r/min, 5 min), and washed with phosphate-buffered saline (PBS). Next, the cells were resuspended in 500 μL of binding buffer (10 mM 4-(2-hydroxyethyl)-1-piperazineethanesulfonic acid (HEPES)/NaOH (pH 7.4), 140 mmol/L NaCl, or 2.5 mmol/L CaCl_2). After a 15-min incubation at room temperature in the dark, FCM was performed to detect apoptosis in each group.

Measurement of ROS

Intracellular accumulation of ROS was measured using a dichloro-dihydro-fluorescein diacetate (DCFH-DA) assay (Nanjing KeyGen Biotech). Cells were treated with DMC (40 $\mu\text{mol/L}$), UVB (50 mJ/cm^2), DMC-PDT (40 $\mu\text{mol/L}$ and 50 mJ/cm^2 , respectively); DMC was precultured for 12 h before UVB irradiation, or DMC-PDT–N-acetyl-L-cysteine (NAC; 40 $\mu\text{mol/L}$, 50 mJ/cm^2 , and 5 mmol/L, respectively). The UVB irradiation occurred following DMC preincubation. NAC was added 2 h prior to irradiation. Following treatment, cells were harvested, washed twice with PBS, and incubated with 10 $\mu\text{mol/L}$ DCFH-DA for 20 min. Cells were washed three times with PBS, resuspended in 0.5 mL PBS, and analyzed by FCM for ROS changes.

Analysis of mitochondrial potential

A431 and HaCaT cells were treated with DMC, UVB, or both agents combined. After treatment, cells were harvested and incubated with Rhodamine 123 (5 $\mu\text{g/mL}$; Nanjing KeyGen Biotech) for 10 min at 37°C in 5% CO_2 . The cells were washed three times with DMEM (without FBS), then resuspended in 0.5 mL of DMEM (without FBS), and incubated at 37°C in 5% CO_2 for 1 h. The Rhodamine 123 signal was measured in the FL1-H channel. Assays were performed in duplicate wells.

Hoechst 33258 DNA staining

A431 and HaCaT cells were seeded in six-well plates and treated with DMC (40 $\mu\text{mol/L}$), UVB (50 mJ/cm^2), or both agents combined. Cells treated with DMEM served as controls. After treatment, the supernatant was discarded and the cells washed twice with PBS before being incubated with Hoechst 33258 (Nanjing KeyGen Biotech) for 5–10

min at room temperature in the dark, then washed twice with PBS, and examined under a fluorescence microscope (Olympus Optical Co. Ltd., Japan).

Western blot analysis

Cells were lysed on ice and centrifuged at 15,000 r/min at 4°C for 20 min. Supernatants were collected and protein concentrations were measured by bicinchoninic acid (BCA) protein assay (Beyotime, China). All of the samples were boiled at 100°C for 5 min. Equal amounts of protein were resolved on 12% sodium dodecyl sulfate–polyacrylamide gel electrophoresis (SDS-PAGE) gels and then transferred to nitrocellulose (NC) membranes. Membranes were blocked with 5% skim milk for 2 h at room temperature and then incubated with primary antibodies (anti-Bcl-2, anti-Bax, anti-caspase-9, anti-cytochrome *c*, anti-NF- κ B, anti-Mcl-1, and anti-caspase-3 (Bioworld Technology, China); anti-glyceraldehyde 3-phosphate dehydrogenase (GAPDH) and anti-P53 (Santa Cruz Biotechnology, USA)) at 4°C overnight. The next day, NC membranes were washed three times with Tris-buffered saline with Tween 20 (TBST) and incubated with corresponding horseradish peroxidase (HRP)-conjugated secondary antibodies (anti-rabbit IgG and anti-mouse IgG; Bioworld Technology) at room temperature for 2 h. NC membranes were then washed three times with TBST and signals detected with SuperSignal ECL (Pierce, USA).

Statistical analysis

SPSS 19.0 software was used for all the statistical analysis. Values are expressed as mean \pm SD. One-way analysis of variance (ANOVA) or Student's *t*-test was performed. The value of $p < 0.05$ was considered statistically significant.

Acknowledgements

Y.X. and Q.H. contributed equally to this work. G.J. and Y.X. contributed reagents/materials/analysis tools and conceived and designed the experiments. P.Z. and Q.H. performed the experiments. P.Z., Q.H., W.W.G., and L.Z.Z. analyzed the data. G.J., Y.X., P.Z., and Q.H. wrote the article.

Declaration of conflicting interests

The author(s) declared no potential conflicts of interest with respect to the research, authorship, and/or publication of this article.

Funding

The author(s) disclosed receipt of the following financial support for the research, authorship, and/or publication of this article: This study was supported by Jiangsu Provincial Medical Talent Foundation and the Department of Science and Technology of Xuzhou (No.KC15SH010).

References

- Smoller BR. Squamous cell carcinoma: from precursor lesions to high-risk variants. *Mod Pathol* 2006; 19: S88–S92.
- García-Zuazaga J and Olbricht SM. Cutaneous squamous cell carcinoma. *Adv Dermatol* 2008; 24: 33–57.
- Palme CE, MacKay SG, Kalnins I, et al. The need for a better prognostic staging system in patients with metastatic cutaneous squamous cell carcinoma of the head and neck. *Curr Opin Otolaryngol Head Neck Surg* 2007; 15: 103–106.
- Kyrgidis A, Tzellos TG, Kechagias N, et al. Cutaneous squamous cell carcinoma (SCC) of the head and neck: risk factors of overall and recurrence-free survival. *Eur J Cancer* 2010; 46(9): 1563–1572.
- Mateus C. Cutaneous squamous cell carcinoma. *Rev Prat* 2014; 64(1): 45–52.
- Dessinioti C, Tzannis K, Sypsa V, et al. Epidemiologic risk factors of basal cell carcinoma development and age at onset in a Southern European population from Greece. *Exp Dermatol* 2011; 20: 622–626.
- Roewert-Huber J, Lange-Asschenfeldt B, Stockfleth E, et al. Epidemiology and aetiology of basal cell carcinoma. *Br J Dermatol* 2007; 157(Suppl. 2): 47–51.
- Wang X, Li J, Li L, et al. Photodynamic therapy-induced apoptosis of keloid fibroblasts is mediated by radical oxygen species in vitro. *Clin Lab* 2015; 61(9): 1257–1266.
- Sharma C, Deutsch I and Horowitz DP. Patterns of care and treatment outcomes for elderly women with cervical cancer. *Cancer* 2012; 118: 3618–3626.
- Mtiller K and Meineke V. Advances in the management of localized radiation injuries. *Health Phys* 2010; 98: 843–850.
- Tsukagoshi S. Development of a novel photosensitizer, talaporfin sodium, for the photodynamic therapy (PDT). *Gan To Kagaku Ryoho* 2004; 31: 979–985.
- Oseroff A. PDT as a cytotoxic agent and biological response modifier: implications for cancer prevention and treatment in immunosuppressed and immunocompetent patients. *J Invest Dermatol* 2006; 126: 542–544.
- Baptista J, Martinez C, Leite L, et al. Our PDT experience in the treatment of non-melanoma skin cancer over the last 7 years. *J Eur Acad Dermatol Venereol* 2006; 20: 693–697.
- Cal Morton, Szeimies RM and Sidoroff A. European guidelines for topical photodynamic therapy, part 1: treatment delivery and current indications—actinic keratoses, Bowen's disease, basal cell carcinoma. *J Eur Acad Dermatol Venereol* 2013; 27: 536–544.
- Shi J, Liu Y and Wang L. A tumoral acidic pH-responsive drug delivery system based on a novel photosensitizer (fullerene) for in vitro and in vivo chemo-photodynamic therapy. *Acta Biomater* 2014; 10: 1280–1291.
- Jäger R, Lowery RP, Calvanese AV, et al. Comparative absorption of curcumin formulations. *Nutr J* 2014; 13: 11.
- Lai CS, Chen YY, Lee PS, et al. Bisdemethoxycurcumin inhibits adipogenesis in 3T3-L1 preadipocytes and suppresses obesity in high-fat diet-fed C57BL/6 mice. *J Agric Food Chem* 2016; 64: 821–830.
- Lin SS, Lai KC and Hsu SC. Curcumin inhibits the migration and invasion of human A549 lung cancer cells through the inhibition of matrix metalloproteinase-2 and -9 and Vascular Endothelial Growth Factor (VEGF). *Cancer Lett* 2009; 285: 127–133.

19. Chen HW, Lee JY and Huang JY. Curcumin inhibits lung cancer cell invasion and metastasis through the tumor suppressor HLJ1. *Cancer Res* 2008; 68: 7428–7438.
20. Hsu CH and Cheng AL. Clinical studies with curcumin. *Adv Exp Med Biol* 2007; 595: 471–480.
21. Hilf R. Mitochondria are targets of photodynamic therapy. *J Bioenerg Biomembr* 2007; 39(1): 85–89.
22. Zhuang S, Demirs JT and Kochevar IE. p38 mitogen-activated protein kinase mediates bid cleavage, mitochondrial dysfunction, and caspase-3 activation during apoptosis induced by singlet oxygen but not by hydrogen peroxide. *J Biol Chem* 2000; 275(34): 25939–25948.
23. Jiang L, Li L, Geng C, et al. Monosodium iodoacetate induces apoptosis via the mitochondrial pathway involving ROS production and caspase activation in rat chondrocytes in vitro. *J Orthop Res* 2013; 31(3): 364–369.
24. Scott I and Logan DC. Mitochondrial morphology transition is an early indicator of subsequent cell death in Arabidopsis. *New Phytol* 2008; 177(1): 90–101.
25. Zhang H, Gajate C, Yu LP, et al. Mitochondrial-derived ROS in edelfosine-induced apoptosis in yeasts and tumor cells. *Acta Pharmacol Sin* 2007; 28(6): 888–894.
26. Diepgen TL and Mahler V. The epidemiology of skin cancer. *Br J Dermatol* 2002; 146: 1–6.
27. Clayman GL, Lee JJ, Holsinger FC, et al. Mortality risk from squamous cell skin cancer. *J Clin Oncol* 2005; 23: 759–765.
28. Wang YJ, Pan MH, Cheng AL, et al. Stability of curcumin in buffer solutions and characterization of its degradation products. *J Pharm Biomed Anal* 1997; 15(12): 1867–1876.
29. Anand P, Kunnumakkara AB, Newman RA, et al. Bioavailability of curcumin: problems and promises. *Mol Pharm* 2007; 4(6): 807–818.
30. Yodkeeree S, Chaiwangyen W, Garbisam S, et al. Curcumin, demethoxycurcumin and bisdemethoxycurcumin differentially inhibit cancer cell invasion through the down-regulation of MMPs and uPA. *J Nutr Biochem* 2009; 20: 87–95.
31. Phipps MA and Mackin LA. Application of isothermal microcalorimetry in solid state drug development. *Pharm Sci Technol Today* 2000; 3: 9–17.
32. Jayaprakasha GK, Jaganmohan Rao L and Sakariah KK. Antioxidant activities of curcumin, demethoxycurcumin and bisdemethoxycurcumin. *Food Chem* 2006; 98: 720–724.
33. Zhang LJ, Wu CF, Meng XL, et al. Comparison of inhibitory potency of three different curcuminoid pigments on nitric oxide and tumor necrosis factor production of rat primary microglia induced by lipopolysaccharide. *Neurosci Lett* 2008; 447: 48–53.
34. Singh S and Aggarwal BB. Activation of transcription factor NF-kappa B is suppressed by curcumin (diferuloylmethane) [corrected]. *J Biol Chem* 1995; 270: 24995–25000.
35. Han SS, Chung ST, Robertson DA, et al. Curcumin causes the growth arrest and apoptosis of B cell lymphoma by downregulation of egr-1, c-myc, bcl-XL, NF-kappaB and p53. *Clin Immunol* 1999; 93: 152–161.
36. Jobin C, Bradham CA, Russo MP, et al. Curcumin blocks cytokine-mediated NF-kappa B activation and proinflammatory gene expression by inhibiting inhibitory factor I-kappa B kinase activity. *J Immunol* 1999; 163: 3474–3483.
37. Ukaji T and Umezawa K. Novel approaches to target NF-kB and other signaling pathways in cancer stem cells. *Adv Biol Regul* 2014; 56: 108–115.
38. Kunnumakkara AB, et al. Curcumin potentiates antitumor activity of gemcitabine in an orthotopic model of pancreatic cancer through suppression of proliferation, angiogenesis, and inhibition of nuclear factor-kappaB-regulated gene products. *Cancer Res* 2007; 67: 3853–3861.
39. Pande D, Karki K, Negi R, et al. NF-kB p65 subunit DNA-binding activity: association with depleted antioxidant levels in breast carcinoma patients. *Cell Biochem Biophys* 2013; 67(3): 1275–1281.
40. Brenner D and Mak TW. Mitochondrial cell death effectors. *Curr Opin Cell Biol* 2009; 21: 871–877.
41. Ghiotto F, Fais F and Bruno S. BH3-only proteins: the death-puppeteer's wires. *Cytometry A* 2010; 77: 11–21.
42. Czabotar PE, Lessene G, Strasser A, et al. Control of apoptosis by the BCL-2 protein family: implications for physiology and therapy. *Nat Rev Mol Cell Biol* 2014; 15: 49–63.
43. Ghate NB, Hazra B and Sarkar R. Alteration of Bax/Bcl-2 ratio contributes to Terminalia belerica-induced apoptosis in human lung and breast carcinoma. *In Vitro Cell Dev Biol Anim* 2014; 50: 527–537.
44. Raisova M, Hossini AM, Eberle J, et al. The Bax/Bcl-2 ratio determines the susceptibility of human melanoma cells to CD95/Fas-mediated apoptosis. *J Invest Dermatol* 2001; 117: 333–340.
45. Ding WX, Ni HM and DiFrancesca D. Bid-dependent generation of oxygen radicals promotes death receptor activation-induced apoptosis in murine hepatocytes. *Hepatology* 2004; 40: 403–413.
46. Stepien A, Izdebska M and Grzanka A. The types of cell death. *Postepy Hig Med Desw* 2007; 61: 420–428.
47. Boatright KM and Salvesen GS. Mechanisms of caspase activation. *Curr Opin Cell Biol* 2003; 15: 725–731.
48. Cain K, Brmton SB and Langlais C. Apaf-1 oligomerizes into biologically active approximately 700-kDa and inactive approximately 1.4-MDa apoptosome complexes. *J Biol Chem* 2000; 275: 6067–6070.
49. Balasubramanian S and Eckert RL. Curcumin suppresses API transcription factor-dependent differentiation and activates apoptosis in human epidermal keratinocytes. *J Biol Chem* 2007; 282: 6707–6715.
50. Viaconti R and D'Adamio L. Functional cloning of genes regulating apoptosis in neuronal cells. *Methods Mol Biol* 2007; 399: 125–131.
51. Kuribayashi K, Mayes PA and El-Deiry WS. What are caspases 3 and 7 doing upstream of the mitochondria? *Cancer Biol Ther* 2006; 5: 763–765.
52. Loekshin RA. Programmed cell death: history and future of a concept. *J Soc Biol* 2005; 199: 169–173.
53. Donepudi M, Mac Sweeney A, Briand C, et al. Insights into the regulatory mechanism for caspase-8 activation. *Mol Cell* 2003; 11: 543–549.